

The physical characteristics of a SLIC-EPID for transmitted dosimetry

M. Mohammadi^{1,2,3*} and E. Bezak^{1,2}

¹*School of Chemistry and Physics, The University of Adelaide, Adelaide, SA 5000, Australia*

²*Department of Medical Physics, Royal Adelaide Hospital, Adelaide, SA 5000, Australia*

³*Department of Medical Physics, Hamedan University of Medical Sciences, Hamedan, Iran*

ABSTRACT

Background: Electronic Portal Imaging Devices (EPIDs) have found an outstanding position for treatment verification in radiation therapy. Several physical characteristics of Scanning Liquid filled Ionization Chamber EPID (SLIC-EPID) including: extra build-up layer, reproducibility and uniformity, and noise level were investigated.

Materials and Methods: To determine the extra build-up layer to reach the electronic equilibrium, 1-30 mm white water materials (RW3) were placed on the EPID cover and the variation of pixel values were investigated. To assess the short term reproducibility, a series of 10 consecutive Electronic Portal Images (EPIs) were acquired. The variation of pixel values were then determined in irradiated field using MATLAB software. For long term reproducibility, the described above experiment was then repeated seven times. To determine the noise level in EPID images, 10 consecutive flood images were acquired. The measurement was repeated after two days during a fortnight.

Results: 5 mm of RW3 material was found to increase the pixel values to the maximum possible. No significant variation was observed between the maximum thickness of build-up layer required for the central axis and peripheral points. For reproducibility measurements, no systematic variation was observed between mean, maximum and minimum acquired pixel values. Both the long-term and short term reproducibility was found to be less than 1%. The noise level was generally less than 1% and this can be referred as an acceptable dose level.

Conclusion: The physical characteristics, measured in this work, suggest that the SLIC-EPID can be used for dosimetry. However, for a particular linac energy and EPID image acquisition mode, the extra build-up layer thickness must be known for the EPID to be used for dosimetric purposes. *Iran. J. Radiat. Res., 2005; 2 (4): 175-183*

Keywords: *SLIC-EPID, physical characteristics, portal dosimetry, transmitted dosimetry.*

INTRODUCTION

Electronic Portal Imaging Devices (EPIDs) were initially introduced for positioning verification (Leong 1986, van Herk *et al.* 1988, Graham *et al.* 1991, Kirby

et al. 1993, Kaatee *et al.* 2002). They have recently been used for dosimetric purposes, relying on a conversion from Electronic Portal Image (EPI) pixel values to dose (Essers *et al.* 1995, Heijmen *et al.* 1995, Kirby *et al.* 1995, Zhu *et al.* 1995, Boellaard *et al.* 1996, Essers *et al.* 1996, Hansen *et al.* 1996, Symonds-Taylor *et al.* 1997, Parsaei *et al.* 1998, Pasma *et al.* 1998, Bogaerts *et al.* 2000). EPIDs can also be used for quality assurance tasks such as the assessment of radiation field symmetry and flatness; verification of the Multi-Leaf Collimator (MLC)

* **Corresponding author:**

M. Mohammadi, Department of Medical Physics, Royal Adelaide Hospital, North Terrace, Adelaide, SA 5000, Australia.

Fax: +61 8 82225937

E-mail: Mahamma@mail.rah.sa.gov.au

position and leaf speed; and the coincidence between light field and radiation field (Boyer *et al.* 1992, Kirby *et al.* 1995, Curtin-Savard *et al.* 1997, Webb 1997, Boellaard *et al.* 1998, Dunscombe *et al.* 1999, Liu *et al.* 2002).

The need for an extra build-up layer in order to achieve electronic equilibrium in the EPID sensitive layer was assessed (Boellaard *et al.* 1996, Essers *et al.* 1996). Using an appropriate extra build-up layer, Boellaard *et al.* showed that SLIC-EPIDs are capable of measuring the transmitted dose rate within $\pm 3\%$ of the ionization chamber results (Boellaard *et al.* 1996). Parsaei *et al.* showed that in the absence of an extra build-up layer, there is a 10 % deviation between measured and calculated dose values, compared to the 16 % deviation for same conditions in Boellaard *et al.*'s study (Parsaei *et al.* 1998). The use of an extra build-up layer in the fluoroscopic EPID (Pasma *et al.* 1998) and amorphous silicon EPID (a-Si EPID) (Greer *et al.* 2003) for accurate dosimetry has also been reported.

The reproducibility of dose response characteristics must be well understood if EPIDs are used to measure dose for therapeutic purposes. Improvement of this factor may lead to the decrease of uncertainties of dose values calculated using EPIDs. Despite the increase in the use of EPIDs for dosimetric purposes in recent years, only a few works have addressed the reproducibility, including the short and long term reproducibility of the dose response characteristics. The reproducibility of an EPID can be affected by several factors such as detector and ambient temperature, warm up time, source-detector distance, etc. Although several Quality Assurance (QA) protocols are proposed for EPIDs, they are not recommended for EPID, used for dosimetric issues (Low *et al.* 1996, Rajapakshe *et al.* 1996).

The evaluation of physical characteristics of the EPID is important if the EPIDs are to be used for dosimetric purposes. For camera-based EPIDs, a good stability in the dose response characteristics of 0.4 % was reported by

Heijmen *et al.* (1995). Pasma *et al.* showed that the short term reproducibility, the variation in average measurements using the same measuring technique, of measurements is less than 0.2 % for the 6 MV photon beam (Pasma *et al.* 1998). The reproducibility of dose response characteristics for SLIC-EPIDs has been assessed in several studies. For instance, Essers *et al.* reported that SLIC-EPIDs have reliable long term stability, better than 1 % over three months (Essers *et al.* 1995). The reproducibility was also reported to be better than 1 % over a period of two years (Louwe *et al.* 2004). The reproducibility for an amorphous Silicon EPIDs (a-Si EPIDs) was recently assessed. It was reported less than 0.8 % (1 SD) for an Intensity Modulated Radiation Therapy (IMRT) field over a period of one month (Greer *et al.* 2003). The stability, which represents variation of EPID pixel values due to elapsed time, was reported less than 1 % and 3 % over a five month period for 6 MV and 15 MV, respectively (Menon *et al.* 2004) on the central axis of radiation field. The maximum short and long term reproducibility was reported less than 2 % for static and dynamic field delivery (Van Esch *et al.* 2004). Both the short-term and long-term reproducibility were reported in several studies (Essers *et al.* 1995, Boellaard *et al.* 1996, Louwe *et al.* 2004), but there is no evidence for uniformity evaluation in the literature review.

Image quality can be defined in terms of image noise, which limits low contrast resolution, and spatial resolution. For instance, in conventional radiography, greater attenuation in thicker patients/absorbers means that fewer photons can construct the image, resulting in an increase in noise level. In the other words, the noise level can be categorized as physical characteristics of imagers.

In this work, the physical characteristics of a SLIC-EPID for portal dosimetry purposes were investigated. Varian SLIC-250 EPID was used for the measurements. The standard automatic calibration procedure of the SLIC-EPID using a

dark image (non-irradiated image) and a flood field image (uniform radiation image) was performed before all experiments and were not repeated during data collection. Initially, the amount of additional build-up layer required was evaluated. Characteristics of acquired EPIDs, including short and long term uniformity and reproducibility, were then assessed. Finally the noise level as an important factor to determine the spatial resolution in several flood images was investigated.

MATERIALS AND METHODS

SLIC-EPID

The SLIC-EPID which is produced commercially as LC250, Portal Vision MK2, consists of 256×256 detectors (Varian Inc., Palo Alto, CA). The detectors contain ionization chambers filled with Is-Octane, an organic liquid. The detector matrix has a sensitive area of $325 \times 325 \times 1 \text{ mm}^3$, contains 256×256 liquid filled ionization chambers and the size of each chamber is $1.27 \times 1.27 \times 1 \text{ mm}^3$. A 1 mm thick stainless steel plate is used as a build-up layer to produce the required electrons to achieve the electronic equilibrium. The central part of detectors, including sensitive area, upper-lower electrode plates and build-up layer, is enclosed between two stabilizing plates used for mechanical support and electrical shielding. For image acquisition, the ionization matrix is scanned at a two rows. The polarizing voltage (400 V) is applied to each two rows. The ionization chamber current in all columns is measured and recorded as pixel values of the whole matrix. The physical characteristics of the SLIC-EPID, used for this work, are shown in table 1.

Linear accelerator

All measurements were performed using the Varian 600CD linac equipped with an 80-leaf MLC, Enhanced Dynamic Wedges (EDW), and a SLIC-EPID. The linac is able to produce standard 6 MV photon beam with a range of

Table 1. The physical operating characteristics of Scanning Liquid Ion Chamber Electronic Portal Imaging Devices (SLIC-EPID) and the linear accelerator used for this study.

Beam Energy	6 MV
Used repetition rates	100, 200, 300, 400, 500 and 600 MU/min
Source to EPID Distance (SED)	110, 115, 120, 125, 130, 135, 140, 150 and 160 cm
Matrix type	Full resolution
Frame averages	1
First Raw wait time	10 ms
Synchronization delay	2000 μ s
Read-out mode	Fast
Start delay	500 ms
Acquisition mode	Standard

dose rates from 100 to 600 MU/min. Image acquisition was performed using available repetition modes (100 - 600 MU/min), with one monitor unit corresponding to a calibrated dose delivery of 1 cGy (1 rad) under the reference conditions (SSD = 100cm, with a $10 \times 10 \text{ cm}^2$ field at depth of d_{max}).

Routine calibration of SLIC-EPID

The standard-automatic calibration of the EPID using a dark image (non-irradiated image) and a flood field image (uniform radiation image) was performed by Portal Vision 6.1 software (Varian Oncology Systems). Measurements were carried out after the system had been switched on for more than 1 hour to ensure that the EPID is in the thermal equilibrium (He *et al.* 1999). All calibration measurements were performed for a nominal $24 \times 24 \text{ cm}^2$ field size on the calibration point. The SLIC-EPID was placed on the Source to EPID Distance (SED) of 140 cm. According to the calibration guideline the linac repetition modes were 100 and 300 MU/min. The SLIC-EPID was set up for fast read-out and full resolution mode.

Investigation of the extra build-up Layer

In order to achieve electronic equilibrium in the EPID sensitive layer, white water, RW3

materials ($\rho = 1045 \text{ g/cm}^3$, PTW Freiburg) of thicknesses varying from 1 mm to 30 mm with a surface area $30 \times 30 \text{ cm}^2$ were placed on top of the EPID cover. A nominal field size of $21.5 \times 21.5 \text{ cm}^2$ at the calibration point (100 cm) and Source to EPID Distance (SED) = 130 cm was set up to cover the maximum surface of RW3 layer. A repetition rate of 300 MU/min was used. The thickness of extra build-up layer in the central point of radiation and 8 off-axis points was investigated. In order to do this, nine 8×8 pixel matrices were selected as shown in figure 1 and the pixel values in each matrix were averaged. The area represented by this pixel array is $0.72 \times 0.72 \text{ cm}^2$ at the isocentre and $1 \times 1 \text{ cm}^2$ at the EPID sensitive layer. This array size was chosen to minimize statistical fluctuation in pixel response with enough spatial resolution (Zhu *et al.* 1995).

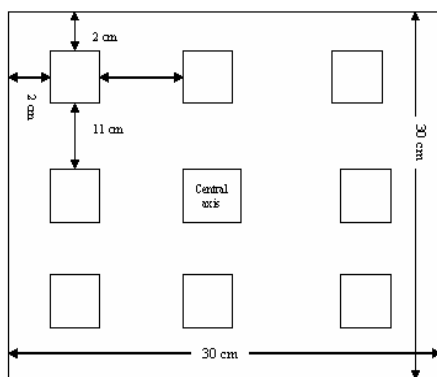


Figure 1. The position of 9 selected matrices.

Reproducibility and uniformity

In order to measure the long term reproducibility, 10 consecutive images were acquired for a field size of $24 \times 24 \text{ cm}^2$ and SED = 130 cm, and dose rate of 300 MU/min. The experiment was then repeated every second day for a period of two weeks to investigate the long-term reproducibility. The first image acquisition was performed following a standard EPID calibration. No calibration was performed for the subsequent acquisitions. The acquired pixel values were then evaluated in 9 points within the irradiated area by selecting and averaging a 10×10 pixel matrix at each point (see figure 1). The acquired Dicom EPIs were analysed to find the values of mean, median, maximum, minimum

as well as standard deviation in each 10×10 matrix. The relative percentage error was calculated as the ratio of maximum-minimum differences and mean pixel values in each selected Region Of Interest (ROI) multiplying by 100.

In order to evaluate the uniformity, the uniformity factor was measured for EPID acquired images using the following equation:

$$\text{Uniformity Factor} = \left[\frac{\text{Max}}{\text{Min}} - 1 \right] \times 100 \quad (1)$$

where Max and Min are the maximum and minimum pixel values in the ROI, respectively (Varian-medical-system 2000). The whole part of a $24 \times 24 \text{ cm}^2$ field size, with a 2-cm discarding of radiation field (a 245×245 matrix of EPID pixel values) was selected as ROI. The data acquisition for short term and long term uniformity was the same as mentioned above for reproducibility.

Noise level

In order to determine the noise level in EPID images, 10 consecutive flood images were acquired for $24 \times 24 \text{ cm}^2$ at Source to EPID Distance SED = 130 cm. The measurement was repeated after two days during a fortnight. The variation of EPID pixel values was obtained over a uniform image on the central axis for a 25×25 matrix ($3.17 \times 3.17 \text{ cm}^2$). After finding the Region Of interest (ROI) in the EPID acquired image, the variation of pixel values was calculated as follows:

$$NL = \max \left\{ 100 \times \sum_{k=1}^{20} \sum_{l=1}^{20} \left[\sum_{i=1}^{i=l} \sum_{j=1}^{j=l} \sqrt{\frac{(PV_{k,l} - PV_{i,j})^2}{PV^2}} \right] \right\} \quad (2)$$

Where NL and PV are the measured noise level and the pixel value, respectively. k and l are the number of pixel values in the ROI. i and j loop over the pixels which are adjacent to the pixel under investigation (Cormack 1993). To process the data MATLAB 6.5 (Mathworks Inc) was used.

RESULTS

Extra build-up layer

Figure 2 shows the variation of SLIC-EPID pixel values for 9 points within a uniform radiation field. The x and y axes are the thickness of extra build-up layer and EPID pixel values, respectively. An increase in pixel values was observed with the increase of build-up layer from zero to 5 mm. A continuous decrease in pixel value was then observed for RW3 thicknesses greater than 5 mm. 5 mm of RW3 material was found to increase the pixel values to the maximum possible, reaching thus the electronic equilibrium. Results also show that there was no significant variation between the maximum thickness of build-up layer required for the central axis and eight peripheral points. Therefore a 5-mm RW3 as additional build-up layer was used for following measurements.

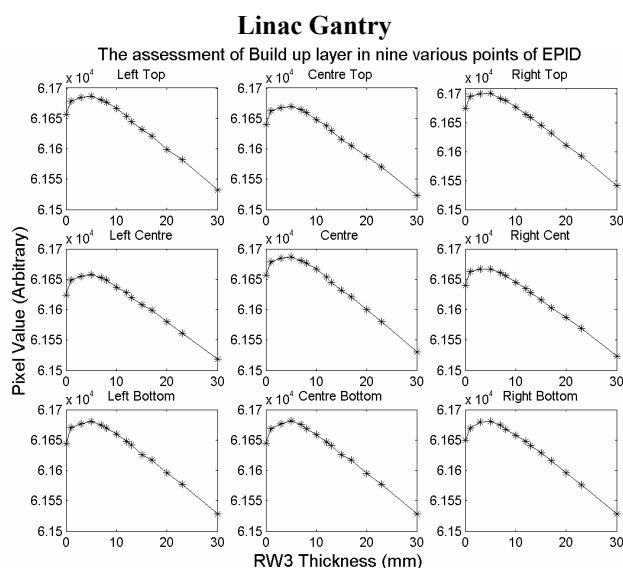
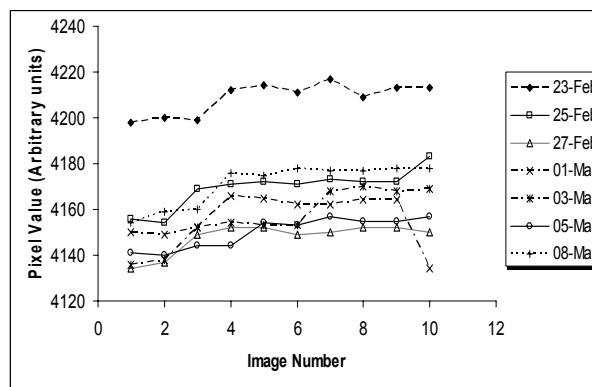


Figure 2. The variation of EPID pixel values with the extra build-up layer thickness. The data for central point and eight peripheral points were acquired with dose rate of 300 MU/min using a 6 MV photon beam, fast read-out and full resolution mode at SED = 140 cm. Each data point is the average of two consecutive measurements.

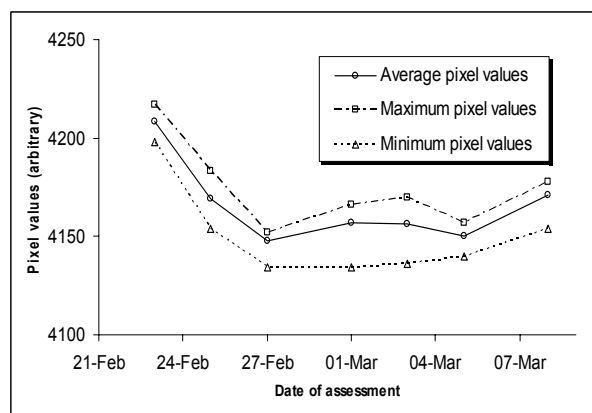
Reproducibility and uniformity

The mean pixel values for a 10×10 matrix, acquired during the study are shown in figure 3.

The mean pixel values did not vary significantly with large number. The average percentage for the relative error was found to be 0.28 % and the maximum relative error observed was 0.37 % during the study.



(a)



(b)

Figure 3. (a) The variation of pixel values of EPID images acquired in 7 series of 10 consecutive images.

(b) The variation of average pixel values of 10 consecutive EPID images on the central axis as a function of time that has elapsed from standard calibration of EPID. All images were acquired in 300 MU/min using 6 MV photon energy, for 24×24 cm² field size at the central axis at SED = 140 cm, 5 mm-RW3 as additional build-up layer, fast read-out and full resolution mode. Each point is the average of two independent and consecutive measurements.

For short-term reproducibility assessment, a 10×10 pixel matrix around the central point of radiation field was selected in 10 consecutive acquired images. The average pixel values in a 10×10 matrix on the central axis are shown in

figure 3(a). For long-term reproducibility assessment, the mean pixel values of a 10×10 matrix on the central axis of 10 daily images acquired consecutively were calculated for 7 series of images acquired within a fortnight with a typical interval of 2 days between acquisitions. The mean pixel values were plotted against the date of assessment. As figure 3(b) shows, no systematic variation was observed between mean pixel values acquired during the study. However, the range of variation can be found from the maximum and minimum pixel values for each measurement. The maximum and minimum acquired pixel values were found to be 4213 and 4136, respectively. The average pixel value was observed to be 4163. The relative error and average standard deviation were consequently found to be 0.82 % and 10.71, respectively.

The obtained results for short term and long term uniformity are plotted versus number of images in figures 4-a and 4-b, respectively. The mean value of short-term uniformity in seven image acquisition series was 2.83 %. The results also showed that the maximum uniformity factor in daily sequentially acquired images is generally around 3.11 % and never exceeds 3.19 %. For long-term uniformity assessment the mean pixel values of 10 daily images acquired consecutively were calculated for 7 series acquired

images. The long-term uniformity obtained from mean pixel values was 2.59 % and maximum long-term uniformity observed was 3.01 %.

Noise level

The measured noise levels and related standard deviations are shown in figure 5. No systematic variation was observed in noise level assessment between 7 series of data sets. The results also show that maximum and minimum

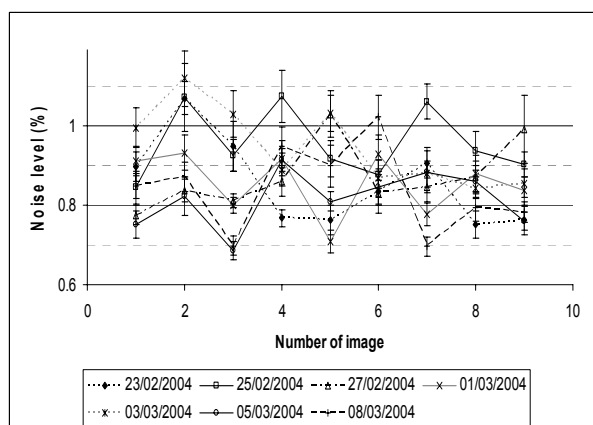
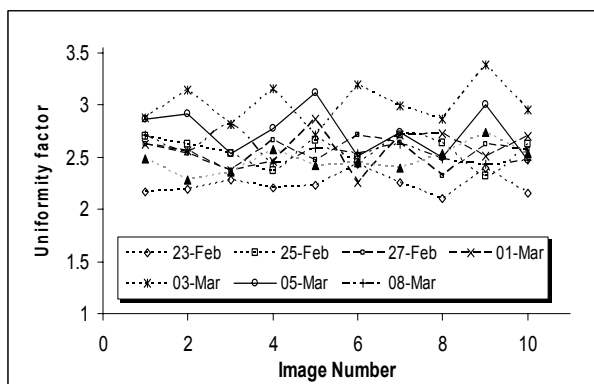
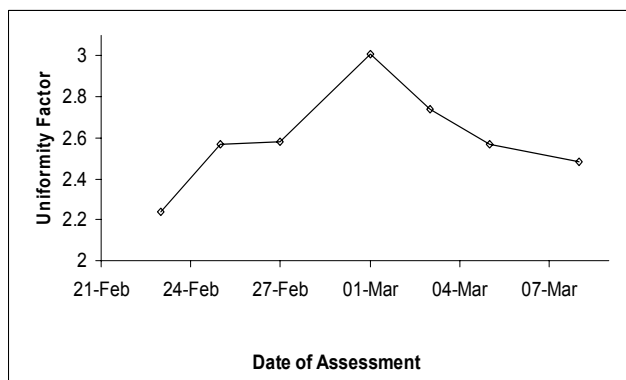


Figure 5. Variation of noise level in 7 series of EPID images. All images were acquired at 300 MU/min using a 6 MV photon beam, for $24 \times 24 \text{ cm}^2$ field size at the central axis at SED = 140 cm, 5-mm additional build-up layer, fast read-out and full resolution mode. Each point is the average of two consecutive measurements.



(a)



(b)

Figure 4. (a) The short-term uniformity of the EPID images calculated for 10 consecutive image acquisitions. (b) The long-term uniformity of EPID images acquired within a fortnight. All images were acquired with 300 MU/min using a 6 MV photon beam, for $24 \times 24 \text{ cm}^2$ field size at the central axis at SED = 130 cm, 5-mm additional build-up layer, fast read-out and full resolution mode. Each point is the average of two consecutive measurements.

noise levels are $1.1 \% \pm 0.07$ and $0.68 \% \pm 0.02$, respectively. The average noise level and standard deviation obtained among 70 processed images were 0.87% and 0.04, respectively.

DISCUSSION

The use of appropriate build-up layer increases the EPID pixel values. The thickness of extra build-up layer, required to reach electronic equilibrium, is dependent on the energy of incident photons. Although, with the increase of average photon energy, the thickness of the build-up layer must be increased, due to the build-up layer dependency on incident radiation energy and the possibility of various available radiation energy for linacs output, it is not possible to cope with this drawback with implementation of constant extra layer in EPIDs. For instance, for linacs which can produce photon beams 6 MV and 25 MV, the additional build-up layer to reach the electronic equilibrium is 8 and 28 mm polystyrene, respectively. These add a weight of 1.3 kg and 4.5 kg to the EPID structure, respectively. However, as the extra build-up layer is required for dosimetric purposes, this deterioration of the image quality must be tolerated (Boellaard *et al.* 1996).

The results showed that both short term and long term reproducibility is less than 1%. They were found to be consistent with data reported for SLIC-EPIDs in the literature (better than 1%) (Essers *et al.* 1995, Zhu *et al.* 1995, Boellaard *et al.* 1996, Louwe *et al.* 2004). According to the consistency between reported reproducibility data and our findings, it is not necessary to perform routine automatic calibration procedure to use EPID for dosimetric purposes. In addition, the short-term and long-term reproducibilities of SLIC-EPID are comparable to fluoroscopic and amorphous silicon EPIDs (less than 1% and 0.8%, respectively) (Pasma *et al.* 1998, Greer *et al.* 2003).

The most significant factor responsible for

this is that the EPID is calibrated in such a way so as to produce uniform response of all liquid ion chambers in the array. This calibration in effect removes the dose variation in the radiation field and produces flat radiation profiles. To a lesser extent, the presence of 1 mm stainless steel in front of the EPID sensitive layer acts as a filter that may attenuate more the low energy X-rays in the peripheral areas (due to angular distribution of X-ray spectrum) compared to central axis (Warkentin *et al.* 2003). As a result of the above mentioned calibration and EPID construction, the use of EPID for dosimetric purposes requires two-dimensional calibration and two-dimensional correction matrix has to be defined.

Due to the noise level measurements obtained from 70 series of data sets, the noise level was generally found to be less than 1% and this will be referred as an acceptable dose level (van Herk 1991, Boyer *et al.* 1992, Casanova Borca *et al.* 2001, Franken *et al.* 2004). It can be concluded that SLIC-EPID images have acceptable noise level and the acquired data sets can be used for dosimetric purposes.

CONCLUSION

The accuracy of portal dosimetry is dependant on the dose response characteristics. Without a comprehensive evaluation of dose response characteristics, EPIDs cannot produce reliable dose measurements. The short-term and long-term reproducibility and noise level, measured in this work, suggest that the SLIC-EPID can be used for dosimetry. However, for a particular linac energy and EPID image acquisition mode, the extra build-up layer thickness and the field size response must be known for the EPID to be used for dosimetric purposes.

ACKNOWLEDGMENT

One of us (MM) gratefully acknowledge the award of scholarship for Ph.D study from

the Iranian Ministry of Health and Medical Education.

REFERENCES

- Boellaard R., Essers M., van Herk M., Mijnheer B.J. (1998). New method to obtain the mid-plane dose using portal in vivo dosimetry. *Int. J. Radiat. Oncol. Biol. Phys.*, **41**: 465-74.
- Boellaard R., van Herk M., Mijnheer B.J. (1996). The dose response relationship of a liquid-filled electronic imaging device. *Med. Phys.*, **23**: 1601-11.
- Bogaerts R., Van Esch A., Reyman R., Huyskens D. (2000). A method to estimate the transit dose on the beam axis for verification of dose delivery with portal images. *Radiother. Oncol.*, **54**: 39-46.
- Boyer A.L., Antonuk L., Fenster A., et al. (1992). A review of electronic portal imaging devices (EPIDs). *Med. Phys.*, **19**: 1-16.
- Casanova Borca V., Pasquino M., Bertodatto M., Tofani S. (2001). A quality control test of the image obtained with electronic portal imaging devices. *Radiol. Med. (Torino)*, **102**: 266-70.
- Cormack J. (1993). An Introduction to image analysis and processing. Adelaide, Flinders Medical Centre.
- Curtin-Savard A. and Podgorsak E.B. (1997). An electronic portal imaging device as a physics tool. *Med. Dosim.*, **22**: 101-5.
- Dunscombe P., Humphreys S., Leszczynski K. (1999). A test tool for the visual verification of light and radiation fields using film or an electronic portal imaging device. *Med. Phys.*, **26**: 239-43.
- Essers M., Boellaard R., van Herk M., Lanson H., Mijnheer B.J. (1996). Transmission dosimetry with a liquid-filled electronic portal imaging device. *Int. J. Radiat. Oncol. Biol. Phys.*, **34**: 931-941.
- Essers M., Hoogervorst B.R., van Herk M., Lanson H., Mijnheer B.J. (1995). Dosimetric characteristics of a liquid-filled electronic portal imaging device. *Int. J. Radiat. Oncol. Biol. Phys.*, **33**: 1265-72.
- Franken E., de Boer J., Barnhoorn J., Heijmen B. (2004). Characteristics relevant to portal dosimetry of a cooled CCD camera-based EPID. *Med. Phys.*, **31**: 2549-51.
- Graham M.L., Cheng A.Y., Geer L.Y., et al. (1991). A method to analyze 2-dimensional daily radiotherapy portal images from an on-line fiber optic imaging system. *Int. J. Radiat. Oncol. Biol. Phys.*, **20**: 613-19.
- Greer P. and Popescu C. (2003). Dosimetric properties of an amorphous silicon electronic portal imaging device for verification of dynamic intensity modulated radiation therapy. *Med. Phys.*, **30**: 1618-27.
- Hansen V.N., Evans P.M., Swindell W. (1996). The application of transit dosimetry to precision radiotherapy. *Med. Phys.*, **23**: 713-21.
- He X., Van Esch A., Reymen R., Huyskens D. (1999). Evaluation of an electronic portal imaging device for transit dosimetry. *Acta. Oncol.*, **38**: 591-6.
- Heijmen B.J., Pasma K.L., Kroonwijk M., et al. (1995). Portal dose measurement in radiotherapy using an electronic portal imaging device (EPID). *Phys. Med. Biol.*, **40**: 1943-55.
- Kaatee R.S., Olofsen M.J., Verstraate M.B., Quint S., Heijmen B.J. (2002). Detection of organ movement in cervix cancer patients using a fluoroscopic electronic portal imaging device and radiopaque markers. *Int. J. Radiat. Oncol. Biol. Phys.*, **54**: 576-83.
- Kirby M. and Williams P. (1995). The use of an electronic portal imaging device for exit dosimetry and quality control measurements. *Int. J. Radiat. Oncol. Biol. Phys.*, **31**: 593-603.
- Kirby M.C. and Williams P.C. (1993). Measurement possibilities using an electronic portal imaging device. *Radiother. Oncol.*, **29**: 237-243.
- Leong J. (1986). Use of digital fluoroscopy as an on-line verification device in radiation therapy. *Phys. Med. Biol.*, **31**: 985-992.

- Liu G., van Doorn T., Bezak E. (2002). Assessment of flatness and symmetry of megavoltage X-ray beam with an electronic portal imaging device (EPID). *Australia's Phys. Eng. Sci. Med.*, **25**: 58-66.
- Louwe R.J., Tielenburg R., van Ingen K.M., Mijnheer B.J., van Herk M.B. (2004). The stability of liquid-filled matrix ionization chamber electronic portal imaging devices for dosimetry purposes. *Med. Phys.*, **31**: 819-27.
- Low D., Klein E., Maag D., Umfleet W., Purdy J. (1996). Commissioning and periodic quality assurance of a clinical electronic portal imaging device. *Int. J. Radiat. Oncol. Biol. Phys.*, **34**: 117-23.
- Menon G. and Sloboda R. (2004). Quality assurance measurements of a-Si EPID performance. *Med. Dosim.*, **29**: 11-17.
- Parsaei H., el-Khatib E., Rajapakshe R. (1998). The use of an electronic portal imaging system to measure portal dose and portal dose profiles. *Med. Phys.*, **25**: 1903-9.
- Pasma K.L., Kroonwijk M., de Boer J.C., Visser A.G., Heijmen B.J. (1998). Accurate portal dose measurement with a fluoroscopic electronic portal imaging device (EPID) for open and wedged beams and dynamic multileaf collimation. *Phys. Med. Biol.*, **43**: 2047-60.
- Rajapakshe R., Luchka K., Shalev S. (1996). A quality control test for electronic portal imaging devices. *Med. Phys.*, **23**: 1237-44.
- Symonds-Taylor J.R.N., Partridge M., Evans P.M. (1997). An electronic portal imaging device for transit dosimetry. *Phys. Med. Biol.*, **42**: 2273-2283.
- Van Esch A., Depuydt T., Huyskens D.P. (2004). The use of an aSi-based EPID for routine absolute dosimetric pre-treatment verification of dynamic IMRT fields. *Radiother. Oncol.*, **71**: 223-34.
- van Herk M. (1991). Physical aspects of a liquid filled ionization chamber with pulsed polarizing voltage. *Med. Phys.*, **18**: 692-702.
- van Herk M. and Meertens H. (1988). A Matrix ionization chamber imaging device for on-line patient setup verification during radiotherapy. *Radiother. Oncol.* **11**: 369-378.
- Varian-medical-system (2000). Portal Vision LC250 MKII system manual. Palo Alto CA.
- Warkentin B., Steciw S., Rathee S., Fallone B.G. (2003). Dosimetric IMRT verification with a flat-panel EPID. *Med. Phys.*, **30**: 3143-55.
- Webb S. (1997). The physics of conformal radiotherapy: Advances in technology. *Bristol, Institute of Physics Publishing*.
- Zhu Y., Jiang X.Q., Van D.y.k.J. (1995). Portal dosimetry using a liquid ion chamber matrix: Dose response studies. *Med. Phys.*, **22**: 1101-1106.